Volume 26
Number 30
14 August 2024
Pages 3991–4122

CrystEngComm

rsc.li/crystengcomm

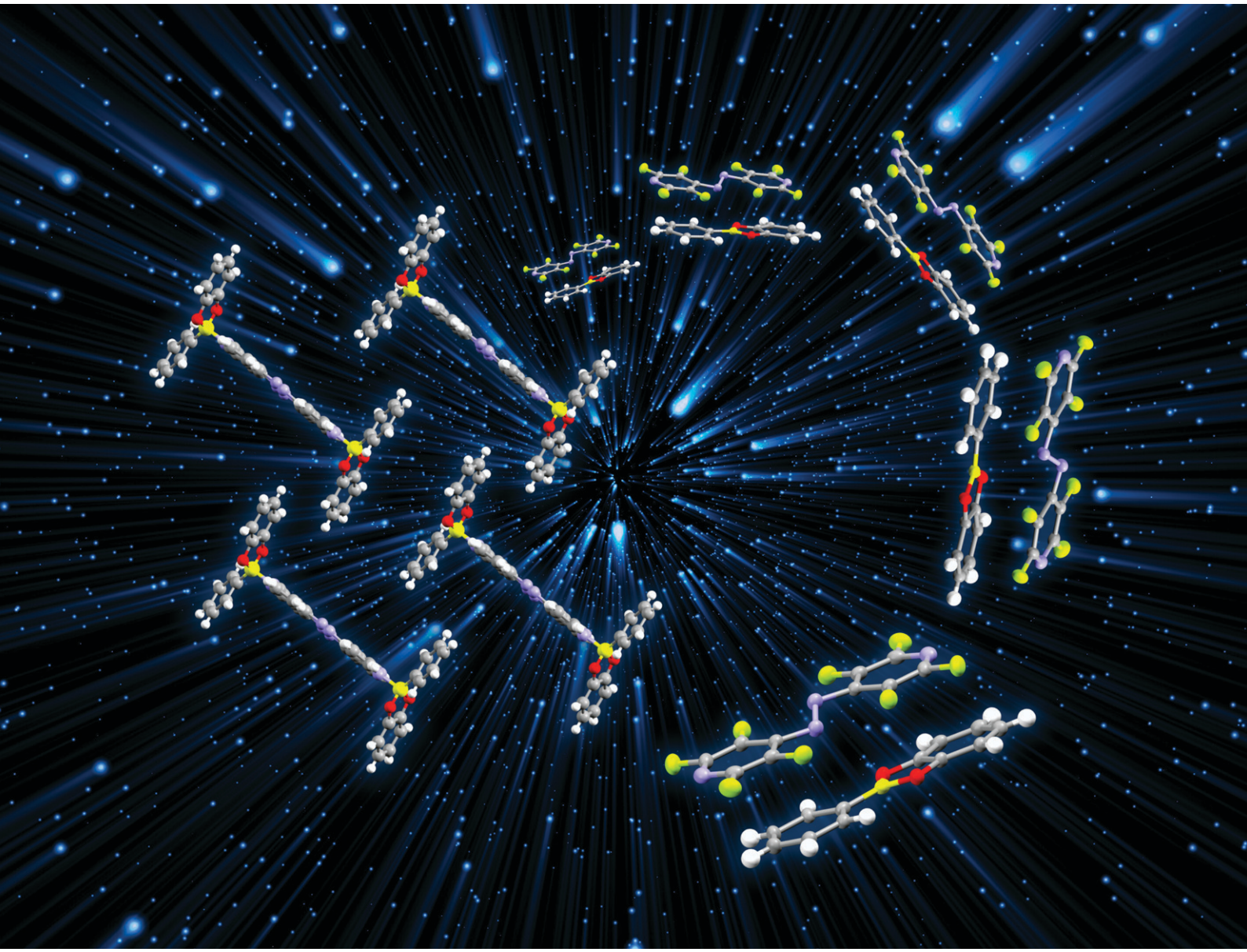

ISSN 1466-8033

ROYAL SOCIETY OF CHEMISTRY

COMMUNICATION

Gonzalo Campillo-Alvarado *et al.*

Co-crystal formation *vs.* boron coordination: fluorination in azopyridines regulates supramolecular competition

CrystEngComm

COMMUNICATION

View Article Online
View Journal | View Issue

Cite this: *CrystEngComm*, 2024, **26**, 4017

Received 18th June 2024,
Accepted 5th July 2024

DOI: 10.1039/d4ce00611a

rsc.li/crystengcomm

Co-crystal formation *vs.* boron coordination: fluorination in azopyridines regulates supramolecular competition†

Jesus Daniel Loya, ‡[a] Sidhaesh A. Agarwal, ‡[a] Nicholas Lutz, [a] Eric W. Reinheimer [b] and Gonzalo Campillo-Alvarado *[a]

Fluorination of azopyridine N-donors regulates the formation of either B ← N coordination adducts or a co-crystal with phenylboronic acid catechol ester. Specifically, the formation of B ← N adducts is promoted by azopyridines with up to four fluorines, while perfluorination affords a co-crystal *via* phenyl–perfluoropyridyl [$\pi\cdots\pi_F$] contacts. Electrostatic potential maps showed supramolecular bonding competition outcomes to be primarily determined by modulation of electron-donating capacity and π surfaces of azopyridine N-donors using fluorination.

Supramolecular bonding competition is a defining feature of self-assembly.[1] Specifically, the ability of a system to undergo self-organization (*i.e.*, spontaneous generations of well-defined architectures based on molecular information stored in molecular building blocks)[2] has profound implications in the fabrication of 2D devices,[3] pharmaceutics,[4] and functional materials.[5] While there has been considerable work on site-specific intermolecular interactions *via* selective self-assembly, studies focusing on the relative hierarchy of competing non-covalent interactions are relatively scarce.[1a,4] Studies have primarily focused on competition between hydrogen and halogen bonds (HB and XB, respectively) in co-crystal formation;[6] achieving control over co-crystallization outcome by appropriate choice of solvent.[6b] However, the increasing number of supramolecular forces used in functional materials demand effective approaches for *a priori* methods to identify dominant forces in supramolecular bonding competition events.[6a]

The ability of organoboron molecules derived from phenylboronic acids to form boron coordination with Lewis bases (*e.g.*, B ← N bond),[7] hydrogen bonding[8] and π-stacking,[9] makes them a suitable platform for systematic studies of supramolecular bonding competition.[10] In this context, organoboronic acid catechol esters are versatile building blocks for functional supramolecular architectures with N-donors.[11] The structures are driven by the directional [B ← N] bond, which results from coordination with an N-containing Lewis base. Work by Adamczyk-Woźniak[12] and Severin[13] has demonstrated the favorable influence of fluorine substituents (*i.e.*, electron-withdrawing groups) installed on phenylboronic catechol esters for the formation of [B ← N] adducts in solution (*i.e.*, acidity of boron center increases).[14] However, to the best of our knowledge, no study has systematically investigated the influence of installing fluorine atoms on the N-donors related to controlling the self-assembly outcome in organoboron compounds. We envisage decreasing the coordinating capacity of N-donors by increasing the number of F-atoms could be used to regulate the outcome of the supramolecular bonding competition.

Here, we demonstrate the outcome of boron coordination and co-crystal formation of phenylboronic acid catechol ester (**PhBE**) can be determined by modulating the fluorination degree of N-donors (Scheme 1). Specifically, we demonstrate differences in Lewis base strength in fluorinated and non-

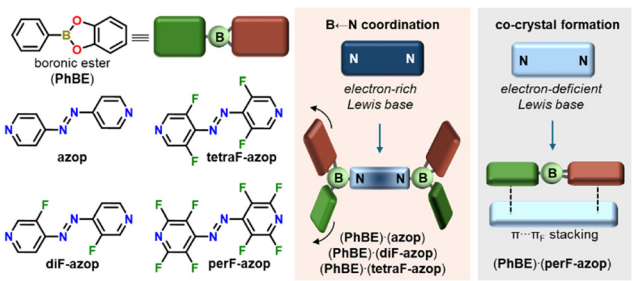

Scheme 1 Supramolecular competition between boron coordination and hydrogen bonding: (left) organoboronic acid catechol ester and azopyridines used in this study, (center) boron coordination with electron-rich Lewis bases, and (right) co-crystal formation with an electron-deficient Lewis base.

[a] *Department of Chemistry, Reed College, Portland, Oregon, 97202, USA. E-mail: gcampillo@reed.edu; Tel: +1 (503) 517 7469*
[b] *Rigaku Oxford Diffraction, The Woodlands, Texas, 77381, USA*

† Electronic supplementary information (ESI) available: Experimental conditions, additional SCXRD data, PXRD data. CCDC 2347086–2347092. For ESI and crystallographic data in CIF or other electronic format see DOI: https://doi.org/10.1039/d4ce00611a

‡ These authors contributed equally.

fluorinated azopyridines: 4,4′-azopyridine (**azop**), difluoro-4,4′-azopyridine (**diF-azop**), tetrafluoro-4,4′-azopyridine (**tetraF-azop**), and perfluorinated, octafluoro-4,4′-azopyridine (**perF-azop**) result in formation of either coordinated complexes (**PhBE**)·(**azop**), (**PhBE**)·(**diF-azop**), and (**PhBE**)·(**tetraF-azop**) or co-crystal (**PhBE**)·(**perF-azop**). Density Functional Theory (DFT) calculations with the ωB97X-D exchange–correlation functional[15] and cc-pVTZ basis set[16] demonstrated the formation of adducts to be driven by the adequate Lewis base strength in N-donors **azop**, **diF-azop**, **tetraF-azop** to promote [B ← N] coordination, while co-crystal formation is primarily due to decreased Lewis base strength in perfluorinated N-donor and electron-deficient **perF-azop** ring, which supports face-to-face phenyl–perfluoropyridyl [$\pi\cdots\pi_F$] stacking with **PhBE**. To the best of our knowledge, regulation of supramolecular competition of boron coordination *versus* co-crystal formation in the solid state *via* fluorination of N-donors is unknown.

To test our hypothesis, we synthesized a series of azopyridines with varying levels of fluorination (**diF-azop**, **tetraF-azop**, **perF-azop**) using an adapted literature procedure (see ESI† for experimental details).[17] The azopyridines (0.15 mmol) were combined with phenylboronic acid (**PhBA**, 0.30 mmol) and catechol (**cat**, 0.30 mmol) in acetonitrile (3 mL). The solutions were gently heated until the solids fully dissolved. Single crystals were observed for all systems after three days of slow evaporation. Phase purity and composition were determined by analysis of powder X-ray diffraction data, and nuclear magnetic resonance (NMR) spectroscopy (see ESI† for experimental, PXRD, and NMR data).

Crystallization of non-fluorinated azopyridine **azop** resulted in the formation of (**PhBE**)·(**azop**) as black blocks. A single crystal X-ray diffraction (SCXRD) study revealed the components to crystallize in the monoclinic space group $P2_1/c$. In the system, two **PhBE** units are orthogonally coordinated *via* [B ← N] bonds (1.682(3) Å) to an **azop** linker forming a H-shaped adduct (Fig. 1a). The **azop** linker is disordered over two positions, likely due to a pedal-like motion.[18] The tetrahedral character (THC) of boron is 73.7%, which is comparable to H-shaped B-based adducts.[7d,19] The twist angle between the pyridyl ring plane with respect to the reference plane defined by the N–B–C atoms (α_{a-d}) is 56.9°, falling in the lower end of reported adducts, which are primarily orthogonal (Fig. 1b).[11] The **azop** motif in the adduct interacts with adjacent **PhBE** motifs on both the pyridyl and phenyl rings *via* [$\pi\cdots\pi$] contacts, forming alternate π-stacks in the *bc*-plane (Fig. 1c). Additional [C–H···O] and [C–H···π] interactions support the aggregation of adjacent adducts, generating an overall herringbone architecture in the *ac*-plane, which is effectively close packed with no voids present (probe radius: 1.2 Å) (Fig. 1d).[20]

Crystallization of **PhBA** and **cat** with **diF-azop**, and **tetraF-azop**, resulted in the formation of adducts (**PhBE**)·(**diF-azop**) and (**PhBE**)·(**tetraF-azop**), respectively. A SCXRD analysis of adducts (**PhBE**)·(**diF-azop**) and (**PhBE**)·(**tetraF-azop**) revealed the systems to crystallize in the monoclinic space group $P2_1/c$

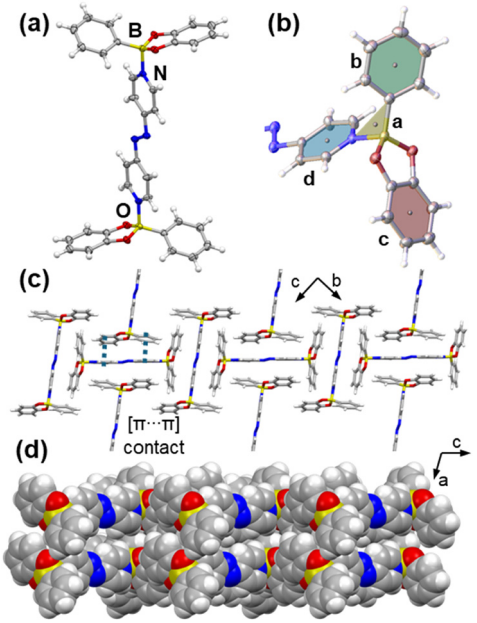

Fig. 1 X-ray structure of (**PhBE**)·(**azop**): (a) edge-to-face [$\pi\cdots\pi$] stacking between **1** and benzene, (b) edge-to-face [$\pi\cdots\pi$] stacking between benzene molecules, (c) van der Waals interactions of **1** in the *bc*-plane, and (d) channels along the *c*-axis. Thermal ellipsoids are shown at a 50% probability level.

as isostructural solids to (**PhBE**)·(**azop**) (Table 1). Specifically, comparable angles, bonds and interaction metrics, and unit cell similarity indices (π)[21] of 0.99, and 0.97 (Tables S1–S7, ESI†), respectively, indicated the adducts to undergo minimal conformational change upon fluorination (Fig. 2a). Increased fluorination in the Lewis base N-donor resulted in larger [B ← N] bond distances and lower THC, indicative of weaker coordination.[22] Face-to-face [$\pi\cdots\pi$] interactions of (**PhBE**)·(**diF-azop**) and (**PhBE**)·(**tetraF-azop**) were weaker than in (**PhBE**)·(**azop**), as shown by the **PhBE** motif sliding away from neighboring azopyridyl linkers (Table 1, Fig. 2b). Conformational flexibility has been documented in host–guest complexes using T-shaped B ← N adducts.[22b] Adducts (**PhBE**)·(**3-diF-azop**) and (**PhBE**)·(**3,5-tetraF-azop**) did not display disorder in the **azop** linker present in (**PhBE**)·(**azop**).

Noteworthy, when perfluorinated azopyridine **perF-azop** was combined with **PhBE** under the same crystallization conditions as the [B ← N] adducts, yellow plates of (**PhBE**)·(**perF-azop**) formed after three days of slow evaporation. A SCXRD analysis revealed the components to crystallize in the triclinic space group $P\bar{1}$. The asymmetric unit contains one-half unit of **PhBE** disordered over two positions with boron as a center of inversion, forming a co-crystal with one half-unit of **perF-azop**. The **PhBE** molecule shows the geometry of the boron atom to be roughly trigonal planar, which contrasts that of boron in (**PhBE**)·(**azop**) (*i.e.*, approximately tetrahedral). The components in (**PhBE**)·(**perF-azop**) primarily interact *via* face-to-face phenyl-perfluoropyridyl [$\pi\cdots\pi_F$] contacts, resulting in columns along the *b*-axis of alternating molecules akin to phenyl–

Table 1 Selected metrics for B ← N adducts and co-crystal

Crystal data[a]	Type of solid	THC (%)	B ← N bond (Å)	π···π contacts (Å)	α_{a-d} rings[c] (°)
(**PhBE**)·(**azop**)	Adduct	73.7	1.682(3)	3.772(1),[a] 3.912(1)[b]	56.9
(**PhBE**)·(**diF-azop**)	Adduct	70.4	1.698(3)	3.826(1),[a] 3.990(1)[b]	56.6
(**PhBE**)·(**tetraF-azop**)	Adduct	66.7	1.714(3)	3.855(1),[a] 4.075(1)[b]	54.9
(**PhBE**)·(**perF-azop**)	Co-crystal	NA	NA	3.682(2),[a] 3.631(2)[b]	NA

[a] $Centroid_{pyr}\cdots centroid_{cat}$. [b] $Centroid_{pyr}\cdots centroid_{phen}$. [c] Dihedral angle ($\alpha$) of a and d rings (see Fig. 1b).

perfluorophenyl systems (Fig. 3a).[23] The alternating molecular arrangement in [π···π_F] stacks is attributed to quadrupolar interactions between electron-rich and electron-deficient rings (Fig. 3b).[24] The results are consistent with observations of structures of fluorinated boronic esters, which show antiparallel dipole–dipole [π···π_F] interactions.[9b] Additional [C–N···H] hydrogen bonds and [C–H···F] contacts support the formation of sheets comprising alternating **PhBE** and **perF-azop** molecules in the *ac*-plane (Fig. 3c).

Rationale for the formation of a B ← N adduct *versus* a co-crystal was provided by Density Functional Theory (DFT) calculations of electrostatic potential maps with the ωB97X-D exchange–correlation functional and cc-pVTZ basis set (Fig. 4).[15,16]

Molecular coordinates were obtained from SCXRD data of synthesized fluorinated azopyridines **diF-azop**, **tetraF-azop**, and **perF-azop**, and reported data for **azop** (CSD refcode: EVESIJ).[25] The analysis revealed that as the level of fluorination increases, the electron density around the nitrogen atoms decreases. For instance, **azop** has a negative band of −160 kJ mol^{-1}, which indicates a higher electron-donating capacity, whereas **perF-azop** has a negative band of −89 kJ mol^{-1}. The Lewis basicity of the nitrogen atom is decreased due to the strong inductive effect of fluorine atoms in the proximity of the nitrogen atom pyridine rings. The increased energy suggests a shift in the electron density from the nitrogen atom by adding electron-withdrawing groups, ultimately leading to co-crystal formation in perfluorinated **perF-azop**. The effect is reminiscent of the prevalence of lone pair···π–hole interaction in perfluorinated pyridine over hydrogen bond formation with water.[26] Moreover, the coordination to the boron center is likely hindered by steric effects and possible repulsion between fluorine and oxygen atoms from catecholates in the boronic ester. Pyridines containing two *ortho* fluorine substituents have also demonstrated reduced electron-donating lone pair capacity.[27]

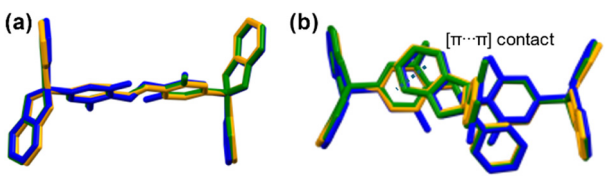

Fig. 2 Overlay of X-ray structures of (**PhBE**)·(**azop**) (orange), (**PhBE**)·(**diF-azop**) (green) and (**PhBE**)·(**tetraF-azop**) (blue): (a) molecular conformations, and (b) slight sliding of [π···π] contacts.

In (**PhBE**)·(**perF-azop**), most of the electron density in the N-donor is pulled towards the fluorine, generating an electron-deficient surface that enables phenyl–perflouropyridyl [π···π_F] contacts.[23]

Hirshfeld surface analysis of the synthesized adducts (**PhBE**)·(**azop**), (**PhBE**)·(**diF-azop**), and (**PhBE**)·(**tetraF-azop**) showed significant contributions of [C···H] contacts at 25.8%, 17.7%, and 17.9%, respectively. The interactions arise primarily from the edge-to-face [π···π] contacts between aromatic rings of **PhBE**. Additional [C···C] contacts in adducts originate from face-to-face [π···π] stacking between azopyridines, and **PhBE**. Co-crystal (**PhBE**)·(**perF-azop**) showed the emergence of repulsive [F···F] contacts (10.1%) on **perF-azop**. The interaction is present in reported perfluorinated compounds[28] and is also observed in the (**PhBE**)·(**tetraF-azop**) adduct (3.2%). A decrease in [C···H] contacts (6.9%) and an increase in [C···C] contacts (11.8%) in the co-crystal (**PhBE**)·(**perF-azop**) are in agreement with an increase of face-to-face phenyl–perfluoropyridyl [π···π_F] contacts. Similarly, [H···H] contacts decrease as the

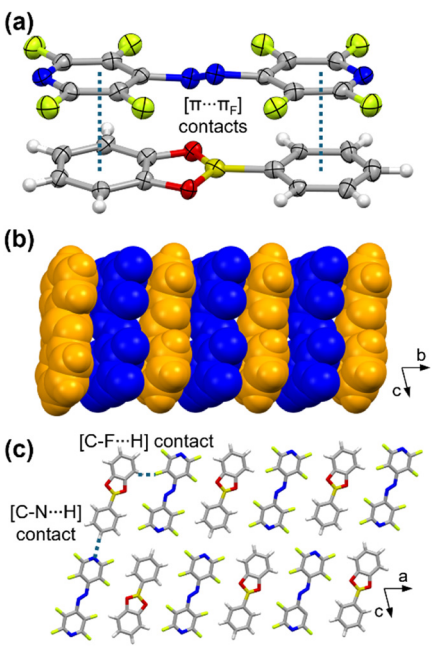

Fig. 3 X-ray structure of (**PhBE**)·(**perF-azop**): (a) [π···π_F] contacts, (b) column of alternating molecules along the *b*-axis, and (c) formation of sheets in the *ac*-plane *via* [C–N···H] and [C–H···F] contacts. Thermal ellipsoids are shown at a 50% probability level.

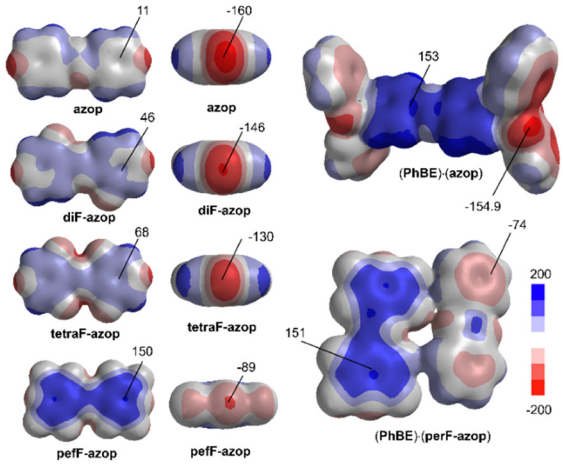

Fig. 4 Electrostatic potential maps of the synthesized azopyridines, coordination complex, and co-crystal. Scale bar and values in kJ mol^{-1}.

fluorination level increases in the adducts and cocrystal (see ESI,† Table S8).

Conclusions

In summary, we have demonstrated that varying the fluorination level in a series of azopyridines (N-donors) regulates the self-assembly of phenylboronic acid catechol ester to form B ← N adducts or a co-crystal. Specifically, the Lewis base strength was higher in N-donors with up to four fluorine atoms, forming B ← N adducts. Perfluorination decreased Lewis base strength and increased the electron-deficient surface, promoting face-to-face phenyl–perfluoropyridyl [$\pi\cdots\pi_F$] contacts in a co-crystal with the boronic ester. Due to the widespread use of organoboron compounds in materials science (*e.g.*, dynamic covalent assemblies)[29] and competing pathways in supramolecular self-assembly, we envision further control using fluorination could generate dynamic boron-based systems with multifunctional properties (*e.g.*, gas storage).[30] In our ongoing work, we are exploring physical and chemical stimuli to control self-assembly pathways in organoboron compounds to form functional solids.

Data availability

The authors confirm that the data supporting the findings of this study are available within the article [and/or] its ESI.†

Author contributions

J. D. L. and S. A. A. carried out investigation, methodology, curation, and validation. N. L. and E. W. R. performed validation, formal analysis, and visualization. J. D. L. performed formal analysis, data curation, and review & editing of the original draft. G. C.-A. contributed by conceptualization, project administration, and writing and reviewing the original draft.

Conflicts of interest

There are no conflicts to declare.

Acknowledgements

We gratefully acknowledge financial support from the M. J. Murdock Charitable Trust (NS-202222588, and FSU-202118942), the National Science Foundation (CHE-2319929), and Reed College (start-up, Stillman Drake and summer funds). J. D. L. appreciates support from the Consortium of Faculty Diversity Postdoctoral Fellowship. We thank Dr. Alan J. Shusterman for helpful discussion on molecular modeling. This study was supported in part by the Betty Moore Foundation.

References

1 (*a*) C. Gunawardana, J. Desper, A. Sinha, M. Đaković and C. Aakeröy, *Faraday Discuss.*, 2017, **203**, 371–388; (*b*) A. J. P. Teunissen, T. F. E. Paffen, G. Ercolani, T. F. A. de Greef and E. W. Meijer, *J. Am. Chem. Soc.*, 2016, **138**, 6852–6860.

2 (*a*) J.-M. Lehn, *Eur. Rev.*, 2009, **17**, 263–280; (*b*) E. Mattia and S. Otto, *Nat. Nanotechnol.*, 2015, **10**, 111–119.

3 M. E. Cañas-Ventura, K. Aït-Mansour, P. Ruffieux, R. Rieger, K. Müllen, H. Brune and R. Fasel, *ACS Nano*, 2011, **5**, 457–469.

4 D. A. Haynes, J. A. Chisholm, W. Jones and W. S. Motherwell, *CrystEngComm*, 2004, **6**, 584–588.

5 (*a*) Y. Wang, P. Meng, A. Brock, Y. Xu, H. Meng, Z. Liu, K. Zhang, J. McMurtrie and J. Xu, *CCS Chem.*, 2024, **6**, 157–164; (*b*) V. Ayzac, Q. Sallembien, M. Raynal, B. Isare, J. Jestin and L. Bouteiller, *Angew. Chem., Int. Ed.*, 2019, **58**, 13849–13853.

6 (*a*) C. B. Aakeröy, C. L. Spartz, S. Dembowski, S. Dwyre and J. Desper, *IUCrJ*, 2015, **2**, 498–510; (*b*) C. C. Robertson, J. S. Wright, E. J. Carrington, R. N. Perutz, C. A. Hunter and L. Brammer, *Chem. Sci.*, 2017, **8**, 5392–5398.

7 (*a*) G. Campillo-Alvarado and L. R. MacGillivray, *Synlett*, 2020, **32**, 655–662; (*b*) G. Campillo-Alvarado, K. P. D'mello, D. C. Swenson, S. V. Santhana Mariappan, H. Höpfl, H. Morales-Rojas and L. R. MacGillivray, *Angew. Chem., Int. Ed.*, 2019, **58**, 5413–5416; (*c*) G. Campillo-Alvarado, C. Li, Z. Feng, K. M. Hutchins, D. C. Swenson, H. Höpfl, H. Morales-Rojas and L. R. MacGillivray, *Organometallics*, 2020, **39**, 2197–2201; (*d*) E. C. Vargas-Olvera, F. J. Salas-Sánchez, A. Colin-Molina, S. Pérez-Estrada, B. Rodríguez-Molina, J. Alejandre, G. Campillo-Alvarado, L. R. MacGillivray and H. Höpfl, *Cryst. Growth Des.*, 2022, **22**, 570–584; (*e*) L. Fornasari, R. Mazzaro, E. Boanini, S. d'Agostino, G. Bergamini, F. Grepioni and D. Braga, *Cryst. Growth Des.*, 2018, **18**, 7259–7263; (*f*) I. J. Jupiter, J. D. Loya, N. Lutz, P. M. Sittinger, E. W. Reinheimer and G. Campillo-Alvarado, *Cryst. Growth Des.*, 2024, DOI: **10.1021/acs.cgd.4c00125**.

8 G. Campillo-Alvarado, A. D. Brannan, D. C. Swenson and L. R. MacGillivray, *Org. Lett.*, 2018, **20**, 5490–5492.

9 (*a*) K. K. Ray, G. Campillo-Alvarado, H. Morales-Rojas, H. Höpfl, L. R. MacGillivray and A. V. Tivanski, *Cryst. Growth Des.*, 2020, **20**, 3–8; (*b*) I. D. Madura, K. Czerwińska, M.

Jakubczyk, A. Pawełko, A. Adamczyk-Woźniak and A. Sporzyński, *Cryst. Growth Des.*, 2013, **13**, 5344–5352; (*c*) C. P. Manankandayalage, D. K. Unruh and C. Krempner, *Dalton Trans.*, 2020, **49**, 4834–4842.

10 (*a*) M. G. Vasquez-Ríos, G. Campillo-Alvarado and L. R. MacGillivray, *Angew. Chem., Int. Ed.*, 2023, **62**, e202308350; (*b*) I. D. Madura, K. Czerwińska and D. Sołdańska, *Cryst. Growth Des.*, 2014, **14**, 5912–5921.

11 N. Luisier, K. Bally, R. Scopelliti, F. T. Fadaei, K. Schenk, P. Pattison, E. Solari and K. Severin, *Cryst. Growth Des.*, 2016, **16**, 6600–6604.

12 A. Adamczyk-Woźniak, M. Jakubczyk, A. Sporzyński and G. Żukowska, *Inorg. Chem. Commun.*, 2011, **14**, 1753–1755.

13 E. Sheepwash, N. Luisier, M. R. Krause, S. Noé, S. Kubik and K. Severin, *Chem. Commun.*, 2012, **48**, 7808–7810.

14 (*a*) A. Adamczyk-Woźniak and A. Sporzyński, *Molecules*, 2022, **27**, 3427; (*b*) J. T. Gozdalik, A. Adamczyk-Woźniak and A. Sporzyński, *Pure Appl. Chem.*, 2018, **90**, 677–702.

15 J.-D. Chai and M. Head-Gordon, *Phys. Chem. Chem. Phys.*, 2008, **10**, 6615–6620.

16 Y. K. Kang and H. S. Park, *Chem. Phys. Lett.*, 2014, **600**, 112–117.

17 N. Iranpoor, H. Firouzabadi, D. Khalili and S. Motevalli, *J. Org. Chem.*, 2008, **73**, 4882–4887.

18 K. M. Hutchins, S. P. Yelgaonkar, B. L. Harris-Conway, E. W. Reinheimer, L. R. MacGillivray and R. H. Groeneman, *Supramol. Chem.*, 2018, **30**, 533–539.

19 G. Campillo-Alvarado, E. C. Vargas-Olvera, H. Höpfl, A. D. Herrera-España, O. Sánchez-Guadarrama, H. Morales-Rojas, L. R. MacGillivray, B. Rodríguez-Molina and N. Farfán, *Cryst. Growth Des.*, 2018, **18**, 2726–2743.

20 C. F. Macrae, I. J. Bruno, J. A. Chisholm, P. R. Edgington, P. McCabe, E. Pidcock, L. Rodriguez-Monge, R. Taylor, J. Streek and P. A. Wood, *J. Appl. Crystallogr.*, 2008, **41**, 466–470.

21 (*a*) P. Bombicz, N. V. May, D. Fegyverneki, A. Saranchimeg and L. Bereczki, *CrystEngComm*, 2020, **22**, 7193–7203; (*b*) P. Bombicz, *IUCrJ*, 2024, **11**, 3–6.

22 (*a*) H. Höpfl, *J. Organomet. Chem.*, 1999, **581**, 129–149; (*b*) G. Campillo-Alvarado, M. M. D'mello, M. A. Sinnwell, H. Höpfl, H. Morales-Rojas and L. R. MacGillivray, *Front. Chem.*, 2019, **7**, 695.

23 (*a*) G. W. Coates, A. R. Dunn, L. M. Henling, J. W. Ziller, E. B. Lobkovsky and R. H. Grubbs, *J. Am. Chem. Soc.*, 1998, **120**, 3641–3649; (*b*) Z. Huang, X. Chen, G. Wu, P. Metrangolo, D. Whitaker, J. A. McCune and O. A. Scherman, *J. Am. Chem. Soc.*, 2020, **142**, 7356–7361.

24 J. Hernández-Trujillo, M. Costas and A. Vela, *J. Chem. Soc., Faraday Trans.*, 1993, **89**, 2441–2443.

25 K. M. Hutchins, K. A. Kummer, R. H. Groeneman, E. W. Reinheimer, M. A. Sinnwell, D. C. Swenson and L. R. MacGillivray, *CrystEngComm*, 2016, **18**, 8354–8357.

26 C. Calabrese, Q. Gou, A. Maris, W. Caminati and S. Melandri, *J. Phys. Chem. Lett.*, 2016, **7**, 1513–1517.

27 M. A. Larsen and J. F. Hartwig, *J. Am. Chem. Soc.*, 2014, **136**, 4287–4299.

28 M. Saccone, A. Pace, I. Pibiri, G. Cavallo, P. Metrangolo, T. Pilati, G. Resnati and G. Terraneo, *CrystEngComm*, 2021, **23**, 7324–7333.

29 X. Li, Y. Zhang, Z. Shi, D. Wang, H. Yang, Y. Zhang, H. Qin, W. Lu, J. Chen and Y. Li, *Nat. Commun.*, 2024, **15**, 1–12.

30 S. S. Sebastian, F. P. Dicke and U. Ruschewitz, *Dalton Trans.*, 2023, **52**, 5926–5934.